International Journal of Artificial Intelligence and Machine Learning
Publisher's Home Page: https://www.svedbergopen.com/
Research Paper Open Access

Feature Extraction With Optimization Model In Plant Disease Detection Using Rule Generation Algorithm And Machine Learning Technique

Nagam Anjineyulu[1] , Dr. S.Nirmal Raj[2]

[1]Research scholar, Department of Computer Science, Sathyabama Institute of Science and Technology, Chennai
anji.amrexamcell@gmail.com
[2]Associate Professor, School of Electrical and Electronics, Sathyabama Institute of Science and Technology, Chennai.
snirmalraj4u@gmail.com nirmalraj.eee@sathyabama.ac.in
Corresponding author : nirmalraj.eee@sathyabama.ac.in

Abstract
Plant diseases pose a serious threat to global food security, and timely detection remains challenging due to the limitations of conventional diagnostic methods, which are often slow, require expert intervention, and lack sufficient accuracy for practical applications. To address these challenges, this study proposes an enhanced image-based detection framework that improves both precision and reliability in identifying plant diseases. The framework integrates Enhanced Feature Fractal Fusion (EFT) for robust feature extraction with a hybrid optimization-driven classification strategy combining Particle Swarm Optimization (PSO) and Levenberg-Marquardt (LM) algorithms. This combination enables effective recognition of complex disease patterns from plant leaf images under diverse conditions. Experimental evaluations demonstrate superior performance, achieving 99% accuracy, 98.99% precision, 99.71% recall, and 99.99% F1-score, outperforming existing state-of-the-art methods. By facilitating rapid and accurate disease identification, the proposed approach supports early intervention, efficient crop management, and sustainable agricultural productivity, making it highly suitable for real-world precision agriculture applications.

Keywords Plant disease detection · feature extraction · Optimization · machine learning algorithms · Levenberg-Marquardt (LM) · feature selection.

1. Introduction

Crop diseases pose a significant threat to global food security, reduce agricultural productivity, and compromise the sustainability of food production systems. Early detection of plant diseases is essential to minimize crop losses, optimize resource management, and ensure sustainable agricultural practices [1]. Over the past decades, agricultural systems have increasingly adopted cutting-edge technology like intelligent algorithms, IoT devices, and automated machinery, resulting in a transition from labor-intensive methods to Precision farming, sometimes referred to as smart farming [2]. Precision agriculture aims to optimize the use of farming resources, including water, pesticides, and labor, while improving crop yield and quality, reducing costs, and supporting environmental sustainability [3]. In this context, quick of plant diseases is critical for early intervention. Conventional techniques that depend on human visual assessment take a lot of time. Furthermore, such approaches are prone to human error and fatigue, which can lead to inconsistent and inaccurate results [4]. To overcome these limitations, image processing techniques have been employed to automatically identify diseases from plant leaf images. Conventional image processing methods, however, require manual feature extraction, which is laborious and may overlook subtle or complex patterns associated with disease symptoms. These techniques also struggle with variations in lighting, background, and environmental noise, limiting their accuracy and generalization to real-world conditions [5]. With varying degrees of efficacy, traditional random forests have been used to identify plant diseases. While these methods can model complex relationships, they still depend on carefully engineered features and perform inconsistently when applied to large-scale or diverse datasets [6]. Moreover, manual feature selection limits scalability, and the accuracy of traditional ML models often declines when tested on images captured under varying field conditions. Overall, plant disease detection faces persistent challenges, including low accuracy in complex disease patterns, reliance on manual feature engineering, poor generalization to field conditions, and limited scalability for large datasets. Previous studies have applied image processing and ML techniques to address these challenges, but these methods still leave gaps in precision, reliability, and practical applicability.

Research gap

Despite significant advances in plant disease detection, existing approaches face persistent limitations. Image processing techniques, while foundational, lack robustness to variations in lighting, background, and leaf orientation, restricting real-world applicability. Traditional ML model and random forests improve classification but rely heavily on handcrafted features, which are insufficient for capturing subtle, overlapping, or complex disease symptoms, particularly under noisy field conditions. Advanced feature-based descriptors enhance accuracy but introduce computational inefficiency and limited generalization, making them unsuitable for real-time deployment in precision agriculture. The proposed hybrid framework integrating EFT with PSO and LM addresses these gaps by automating robust feature extraction, optimizing classifier parameters efficiently, and enhancing generalization across diverse field scenarios. This method overcomes prior limitations by combining high accuracy, computational efficiency, and scalability, enabling reliablefor sustainable crop management.

Key Contributions

- Developed an automated image-based framework for plant disease detection using advanced feature extraction and hybrid optimization-driven classification.
- Enhanced leaf feature representation by integrating Enhanced EFT for improved robustness and discriminative power.
- Applied hybrid PSO-LM algorithms for classification, improving model accuracy, reliability, and early disease detection performance on plant datasets.
- Validated the proposed approach on real-world leaf image datasets, achieving superior results over current state-of-the-art detection methods.
- Enabled rapid, precise, and practical plant disease identification, supporting early intervention, optimized crop management, and sustainable agricultural productivity.

Research is arranged in the following order of organization: Portion 1 presents the introduction. Portion 2 presents the Literature survey. Portion 3 demonstrates the current classification method. Portion 4 focuses on the performance evaluation findings, and Portion 5 provides a conclusion.

2. Literature survey

Deep learning (DL), ML, Fang et al., [7] and image processing approaches have all been extensively researched for plant disease identification; each has unique advantages and disadvantages. Early studies relied Bonkra et al., [8] on image processing methods such as color conversion, Otsu's thresholding, and watershed algorithms for segmenting diseased regions, followed by classifiers like Artificial Neural Networks (ANNs) Mohammed et al., [9]. These approaches demonstrated the feasibility of automated detection, but they required extensive manual feature extraction, were sensitive to lighting and background variations, Thite et al., [10] and lacked scalability for real-world agriculture. To improve upon this, traditional ML models such as SVM, random forests, and KNN were employed to classify diseases in crops like tomato, Liu et al., [11] wheat, and soybean. While these models outperformed purely image-based systems by providing structured classification, Ahmed & Yadav [12] their inability to catch subtle or overlapping symptoms was hampered by reliance on handcrafted features Paul et al., [13], and performance degraded when tested on noisy field images with complex conditions. More advanced methods introduced shape descriptors, Zernike moments, histogram of oriented gradients, and local binary descriptors to improve classification accuracy and automate plant Demilie [14] species identification. While these enhancements offered better disease recognition and taxonomic classification, they still suffered from computational inefficiency, dependence on carefully designed features, and reduced generalization in uncontrolled field environments. At the model architecture level, ResNet50 and Inception-v3 have been contrasted for automated plant disease classification, emphasizing efficiency and accuracy Wang et al., [15]. Hybrid and ensemble models have also played a role, with stacking strategies enhancing potato leaf disease prediction through transfer learning Jha et al., [16]. IoT-assisted frameworks integrated with DL have extended applications into smart agriculture, supporting sustainable crop management (Al-Shahari et al., [17]. Broader surveys have synthesized the state of research, outlining advances and challenges in ML- and DL-based detection Qadri et al., [18]. Real-time CNN-driven frameworks for tomato leaves have demonstrated strong field applicability Khan et al., [19], while DL-based approaches across multiple crops have reinforced the potential of precision agriculture Zhang et al., [20]. In contrast to cutting-edge techniques, Eunice et al., [21] The suggested work improved accuracy and dependability, where DenseNet-121 reached 99.81% accuracy on the PlantVillage dataset, though reliance on controlled images limited real-world applicability. The proposed work introduced the NZDLPlantDisease-v1 dataset with an optimized RFCN model, Saleem et al., [22] achieved 93.80% precision, outperformed default parameters by 19.33%, and showed robustness, though dependence on a specific horticultural dataset restricted broader applicability. The proposed work introduced FieldPlant Moupojou et al., [23] Includes 8,629 annotated leaves in 27 disease classes and 5,170 plantation photos, achieved superior performance over PlantDoc, though dependence on a single dataset restricted wider agricultural applicability. Overall, prior research highlights three key insights: (1) image processing methods established the foundation but lacked robustness; (2) traditional ML approaches provided improvements but remained constrained by feature engineering; and (3) advanced feature-based models offered incremental gains but struggled with scalability and adaptability. Addressing these gaps, the present work proposes a hybrid framework integrating EFT for robust feature extraction with a classification strategy combining PSO and LM algorithms. By balancing high accuracy with computational efficiency, this approach advances beyond existing methods, enabling reliable, scalable, and real-time plant disease identification suitable for sustainable crop management and precision agriculture.

3. Proposed plant disease detection based on feature extraction and optimization model:

Fig. 1 illustrates the complete workflow for plant disease detection, beginning with data collection from crop fields, followed by preprocessing, augmentation, dataset splitting, model training, and testing, ultimately leading to accurate performance evaluation and reliable leaf disease identification. The proposed work uses plant leaves from six different crops in 27 categories to create a deep learning (DL) architecture. The data is transformed into the same dimensions, tested, validated, and trained using various parameters. The method is evaluated using unseen photos from every category. Fig. 1 illustrates the workflow for plant disease detection, beginning with crop field data collection and preprocessing, followed by augmentation, dataset splitting, model training, and testing, ultimately enabling accurate classification, performance analysis, and reliable identification of diseased plant leaves.

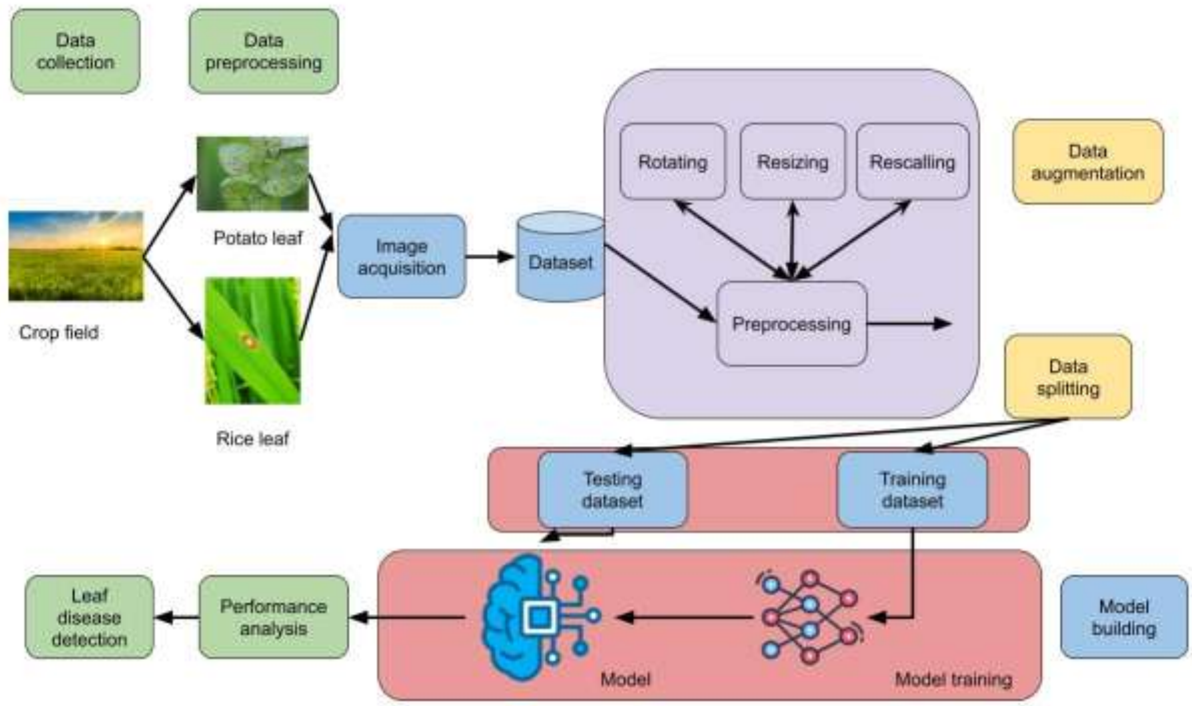

Fig. 1 proposed plant disease detection in feature extraction and optimization model

3.1 Dataset

The purpose of data acquisition is to systematically collect high-quality plant leaf images, ensuring reliable input for preprocessing, feature extraction, and accurate classification in disease detection systems. This research makes use of the rice and potato datasets. The 80:20 setups for the rice and potato datasets indicate that 80% of 20% of the photographs are used for training, with the remaining pictures. The 5932 images in the Rice dataset show there are four distinct rice leaf diseases. 947 images were used for testing and 3785 for training in an 80:20 test-train split. Fig. 2 displays representative photos from the rice dataset. Fig. 2 illustrates rice leaf disease examples: (a) bacterial blight with elongated lesions, (b) brown spot showing small necrotic patches, (c) leaf blast with circular spots, and (d) sheath blight causing wilting, crucial for accurate disease classification.

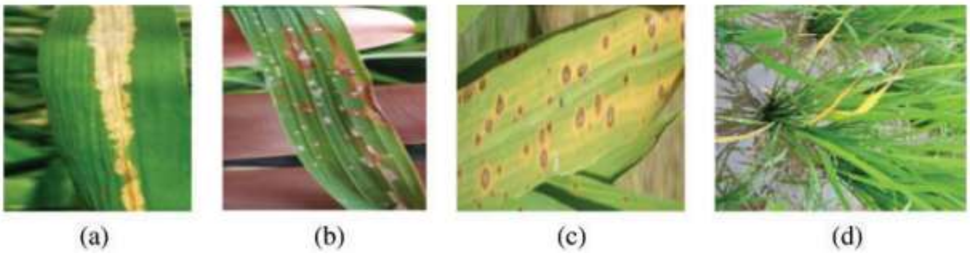

Fig. 2 Sample images of rice leaf image dataset (a) bacterial blight, (b) blast, (c) brown spot, (d) tungro

A set of 1500 photos of potato leaves is used in the investigation. 300 photos were used for testing, whereas 1200 photos were used for training and validation. The quantity of training and testing images in datasets is shown in Table 1. Fig. 3 presents potato leaf samples: (a) early blight characterized by irregular dark lesions, (b) late blight showing brown decayed patches with tissue damage, and (c) a healthy leaf, providing visual distinctions essential for accurate disease recognition and classification. The suggested model's ROC curve. Strong discriminative ability is indicated by the high AUC value of 0.98, which shows that the model can consistently tell healthy leaves from unhealthy ones.

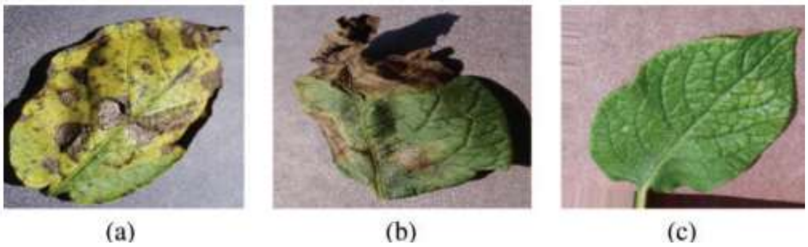

Fig. 3 Sample image of potato leaf diseases (a) early blight, (b) late blight, (c) healthy

Table 1 Plant leaf datasets

Image dataset	Testing images	Classes
Rice dataset	947	04
Potato leaf dataset	300	03

3.2 Enhanced Feature Fractal Fusion (EFT):

Enhanced EFT integrates multi-level fractal features to capture complex texture and structural details, enabling robust, discriminative, and reliable feature representation for accurate plant disease detection. Primary procedures include selecting fractal eigenvalues, segmenting regions of interest, extracting fractal-dimension value features, RPH detection and quantity estimates modeling, and FCM classification.

Following the division of preprocessed images into blocks, Eq. 1 was used to extract the fractal-dimension value features from each image block using the box-counting dimension technique.

$$D_j = \lim_{r\to 0} \frac{\log(N_r)}{-\log(r)} \quad (1)$$

The equation $D_j = \lim_{r\to 0} \frac{\log(N_r)}{-\log(r)}$ defines the fractal dimension, where D_j quantifies structural complexity, rrr represents the scale approaching zero, and N_r denotes the number of non-empty boxes covering the object. Here, $\log(N_r)$ reflects how the object's details vary with scale, while $-\log(r)$ ensures a positive denominator for proper scaling. This formulation captures the self-similarity and irregularity of patterns, making it highly useful in fractal analysis and feature extraction for plant disease detection.

The research analyzes eleven fractal-dimension value statistics of subregional image chunks to select an appropriate eigenvalue for the complete image, considering standard deviation, range, mode, coefficient of variation, interquartile range, moment, skewness, arithmetic mean, and kurtosis.

Fractal Dimension- For a bounded set A in R 0, the Hausdorff–Besicovitch (HB) number, or FD, can be used to characterise its complex geometry. When the topological dimension is strictly less than the HB dimension, the set is a fractal set. The concept of self-similarity is utilized to assess FD.

The Eq. 2 relates fractal geometry parameters. Here, $A(r)$ denotes the measured area at scale r, lg represents the logarithm (base 10), D is the fractal dimension indicating the object's complexity, r is the measurement scale, and K is a proportionality constant reflecting structural characteristics. The term $(2 - D)lg\, r$ explains how the area changes with scale depending on complexity, while $lg\, K$ shifts the relationship based on intrinsic properties. This formulation highlights scale-dependent variations, useful in texture and disease pattern analysis.

$$lg\, A(r) = (2 - D)lg\, r + lg\, K \qquad (2)$$

The equation estimates the fractal dimension D, where M is the number of scales, r_i denotes the i-th measurement scale, $lg\, r_i$ is its logarithm, $A(r)$ represents the measured area at that scale, and $lg\, A(r)$ is its logarithm. The numerator expresses covariance between scale and area, while the denominator reflects variance of scales. This regression-based formulation quantifies structural complexity, enabling precise characterization of texture patterns in plant disease detection. Based on the above Eq. 3 and the linear regression concept.

$$D = 2 - \frac{M\sum_{i=1}^{M} lg\, r_i^{*} gA(r) - \sum_{i=1}^{M} lg\, r_i \sum_{i=1}^{M} lg\, A(r)}{M\sum_{i=1}^{M} (lg\, r_i)^2 - \left(\sum_{i=1}^{M} lg\, r_i\right)^2} \qquad (3)$$

The aforementioned formula demonstrates that number of fractal dimensions are determined following the computation of the surface areas of various sizes. Top surface and two sides of every cube represent surface area of surface, every pixel in remote sensing greyscale image is thought of as a cubic column by Eq. 4

The equation for $A(r)$ represents the fractal area at scale r, where M and N are the image dimensions, $f(i,j)$ is the pixel intensity, and $A_H(i,j)$ denotes local contributions. The base term $M^*N^*r \wedge 2$ accounts for overall image size, while the summation terms capture vertical and horizontal intensity differences $f(i,j) - f(i+1,j)$ and $f(i,j) - f(i,j+1)$, reflecting local texture irregularities. Together, these components quantify structural complexity and variations, enabling effective characterization of disease patterns in plant leaves.

$$A(r) = \sum_{j=1}^{M} \sum_{j=1}^{N} A_H(i,j) + \sum_{j=1}^{M-1} \sum_{j=1}^{N} A_H(i,j) + \sum_{j=1}^{M} \sum_{j=1}^{N-1} A_H(i,j) = M^*N^*r \wedge 2 + r^* \sum_{j=1}^{M-1} \sum_{j=1}^{N} |f(i,j) - f(i+1,j)| + r^* \sum_{j=1}^{M} \sum_{j=1}^{N-1} |f(i,j) - f(i,j+1)| \qquad (4)$$

A fractal-dimensional matrixis created by assigning a dimension value to the convolution centre point, which turns into a crucial feature. Plant diseases disrupt natural leaf vein organization and surface smoothness, creating irregular lesions and texture variations. Fractal features effectively capture these changes by quantifying complexity, irregularity, and self-similarity. Unlike color or edge-based features, fractal dimensions remain robust against scale, orientation, and noise, making them biologically meaningful and reliable indicators of disease progression in real agricultural conditions.

3.3 Particle Swarm Optimization (PSO) integrated with the Levenberg-Marquardt (LM) algorithm:

3.3.1 Levenberg-Marquardt (LM) algorithm:

The LM algorithm is a very effective optimization technique that combines the gradient descent and Gauss-Newton techniques to offer users faster convergence, reliability, and accuracy when training complex classification models. The LM technique was created by Kenneth Levenberg, and revised by Donald Marquardt and provided numerical solutions for cases involving non-linear functions for example: minimize. This type of neural nets training is both fast and tends to always converge. The two other neural net training techniques - Gauss-Newton method and steepest descent algorithm - are also well accepted. The LM algorithm trains a procedure around a dataset in a region where complex curvature occurs and it only changes to steepest descent when curvature is just right.This function assesses the difference between the desired and actual results, or the inconsistency between the NN's true and expected output, using Eq. 5.

$$E(n) = \frac{1}{2}\sum_{k=1}^{m} e_k^2(n);\ e_k(n) = d_k(n) - y_k(n) \qquad (5)$$

Where n is a training epoch, m = number of outputs, d_k = desired (target) output, y_k = actual ANN output and E = mean-squared error surface, $e_k(n)$ = instantaneous error.

Because the error must be calculated layer per layer in a serial fashion, algorithms that employ simple steepest descent minimisation according to first-order minimisation is given as Eq. 6.

$$\Delta W(n) = -\eta * \nabla E(n) + \alpha \Delta W(n-1) \qquad (6)$$

By locally averaging gradient, momentum technique attempts to obtain some curvature data about error surface. Optimization strategies that employ another method for minimizing error E(n) by using Eq. 7 depend on the cost function or performance index $J(w)$'s second-order derivative.

$$J(W_{n+1}) = J(W) + \Delta W \nabla J(w) + \frac{1}{2}\Delta W \nabla^2 J(w) + \cdots \quad (7)$$

Where $\frac{\partial E(n)}{\partial(W(n))} = \nabla J(w) = g$

where the performance index's gradient is given as Eq. 8

$$\frac{\partial^2 E(n)}{\partial^2(W(n))} = \nabla^2 J(w) = H \quad (8)$$

This method was developed to approach second-order training speed without the need to compute the Hessian matrix. Eq. 9 provides the performance function, which is represented by the sum of squares in the following Hessian matrix.

$$H(n) = J^T(n)J(n) \quad (9)$$

3.2.2Particle Swarm Optimization (PSO)

PSO is a population-based optimization technique inspired by swarm intelligence, efficiently exploring solution spaces to enhance parameter tuning, improve accuracy, and optimize performance in computational models. The research proposes a binary selection method for feature selection in PSO, with a population size of 70 from a sample space of 1 to 2100. A multi-objective fitness function is used to modify velocity and parameters. Deep neural networks extract over 100 features, and an optimization model is needed to identify dominant features. PSO is promoted by social behaviors and aims to improve knowledge through social interaction, by Eq. 10

$$Vi(t+1) = w * Vi(t) + c1 * ud * [pbesti(t) - Pi(t)] + c2 * ud * [gbest(t) - Pi(t)]$$
$$Pi(t+1) = Pi(t) + Vi(t+1) \quad (10)$$

Where Vi = Velocity, $Vi(t+1)$ = updated Velocity, $Pi(t)$ = Position of particle, w = Inertia weight, $c1, c2$ = Acceleration coefficients, ud = Uniformly distributed random number, $pbest$ = Best position, $gbest$ = Best global position.

The following equation makes use of the wave function in the quantum space particle by Eq. 11

$$|\Psi|^2 dxdydz = Qdxdydz \quad (11)$$

Among these, |Ψ|2 indicates density of a particle's probability of appearing and is square of wave function's module. $dxdydz$ = Infinitesimal volume element. In following equation, Q represents the likelihood density function and meets the normalisation requirements by Eq. 12.

$$\int_{-\infty}^{+\infty} |\Psi|^2 dxdydz = \int_{-\infty}^{+\infty} Qdxdydz = 11. \quad (12)$$

The iteration value is indicated by t among them. The expansion factor for contraction and the quantum PSO variable are indicated by β. This equation defines the mean probability vector $p(t)$ at time t, where n is total samples, $p_i(t)$ are individual probability vectors, and D represents feature dimensions. The following equation and the model work best to prevent premature convergence by Eq. 13.

$$\text{mbest }(t) = \frac{1}{n}\sum_{i=1}^{n} p_i(t) = \left[\frac{1}{n}\sum_{i=1}^{n} p_{i1}(t), \frac{1}{n}\sum_{i=1}^{n} p_{i2}(t), \ldots, \frac{1}{n}\sum_{i=1}^{n} p_{iD}(t)\right] \quad (13)$$

In contrast, n indicates the quantity of particles and pi indicates the ideal placement of ith particles. The following equation's problem-based dimension is resolved by mbest, which determines the average ideal location of n particles. Here, L is step size, β is control parameter, mbest denotes mean best position, x_{id} is current solution, p_{id} is candidate position, u is random uniform variable by Eq. 14.

$$L = 2 \cdot \beta \cdot |\text{ mbest } - x_{id}|,$$
$$x_{id} = p_{id} \pm \beta \cdot |\text{ mbest }_d - x_{id}\Big| \cdot In\left(\frac{1}{u}\right). \quad (14)$$

The following equation, Here, p_{id} is candidate position, p_{gd} is global best, ϕ is weight factor, and $mbest(t)$ is mean best position. This expression defines $mbest(t)$ as a vector of averages. Each component, $\frac{1}{n}\sum_{i=1}^{n}$, represents the mean value of the d-th dimension across all n individuals in D-dimensional space. which describes the quantum PSO particle update Eq. 15.

$$p_{id} = \phi \cdot p_{id} + (1-\phi) \cdot p_{gd},$$
$$\text{mbest }(t) = \frac{1}{n}\sum_{i=1}^{n} P_i(t),$$
$$= \left[\frac{1}{n}\sum_{i=1}^{n} P_{i1}(t), \frac{1}{n}\sum_{i=1}^{n} P_{i2}(t), \ldots, \frac{1}{n}\sum_{i=1}^{n} PD_i(t)\right],$$
$$= \left[\frac{1}{n}\sum_{i=1}^{n} P_{i1}(t), \frac{1}{n}\sum_{i=1}^{n} P_{i2}(t), \ldots, \frac{1}{n}\sum_{i=1}^{n} PD_i(t)\right],$$
$$X_i(t+1) = P_i \pm \beta \cdot |\text{mbest} - X_i(t)\Big| \cdot ln\left(\frac{1}{u}\right) \quad (15)$$

The arbitrary value within [0,1] is indicated by ϕ among them; other variables are comparable to the one described above.

PSO works like a flock of birds searching for food, where each bird represents a possible feature subset. By sharing information and moving toward the best solution, PSO identifies the most relevant features for disease classification. The LM algorithm then fine-tunes the model by adjusting weights to minimize prediction errors. LM combines the speed of gradient descent with the precision of least squares, ensuring greater accuracy and stability. In the proposed pipeline, PSO was used to select the most informative features, while LM optimized classifier parameters to improve performance and reliability.

Combining PSO with LM is advantageous because PSO performs global exploration to identify the most informative feature subsets, while LM provides local refinement by fine-tuning model parameters. This synergy ensures both broad search capability and precise optimization, reducing risks of overfitting or converging to suboptimal solutions. In the proposed framework, PSO was used for feature selection, and LM was applied to optimize the neural network's weights and biases during training, thereby improving classification accuracy and stability.

Table 2 presents PSO hyperparameters, ensuring balanced exploration, convergence, and effective feature selection.

Table 2 Hyperparameter settings for PSO

Hyperparameter	**Value**
Population size	70
Maximum iterations	100
Inertia weight (ww)	0.75
Cognitive parameter (c1c_1)	0.75
Social parameter (c2c_2)	0.75
Velocity update method	Modified with local & global best
Fitness function	Multi-objective

4. Results and discussion

Experimental setup: Training and assessing the dataset samples validates the model. Using a range of leaf images from various crops, a DL-based plant disease detection and classification framework is trained on a PC with an Intel Xenon CPU running 64-bit Windows 10 with 64 GB of RAM and an NVIDIA Quadro P600 GPU with 24 GB of RAM. This Python programming framework makes use of the Tensorflow, Keras, PyTorch, and OpenCV modules from the Anaconda Jupyter Notebook. The photos' input size was 256x256 pixels, and the batch size was set at 32. In this work, a learning rate of 0.001 is used. Since performance becomes nearly saturated after 60 epochs, the number of epochs is set to 100 and the momentum value is set to 0.9.

Data Augmentation- Keras library's Image Data Generator function was utilized to resize and rescale samples, as well as carry out data augmentation techniques. Table 3 highlights the model's performance metrics. The high recall value of 0.95 ensures that most diseased crops are correctly identified, reducing the risk of undetected infections. The precision value of 0.93 indicates that healthy crops are rarely misclassified, minimizing unnecessary interventions. Overall, these figures and metrics collectively demonstrate the resilienceof the proposed model for plant disease detection, and Fig. 4 shows data augmentation results, where (a) is the original diseased leaf and (b–e) represent augmented samples generated through transformations, enhancing dataset diversity and improving model robustness for accurate disease detection and classification.The accuracy and loss curves for training and validation. The close alignment of these curves demonstrates stable convergence, minimal overfitting, and good generalization of the model. The following parameters, which are listed in Table 4, were taken into consideration during the experiments:

Table 3 Experimental parameters setting.

Parameters	**Values**
Learning Rate	. 001
Shearing	-0.3 to +3
Optimizer	Adam
Drop out	0.01
Horizontal flipping	True
Batch Size	32
Zooming	0.5 to 1.5
Rotating	-10 to +10

Validation split	0.2

Table 4 Data augmentation methods as well as their corresponding values

Data augmentation techniques	Value
Rotation	30
Shear	0.1
Height shift	0.2
Width shift	0.2
Zoom	0.3
Fill mode	nearest
Horizontal flip	True

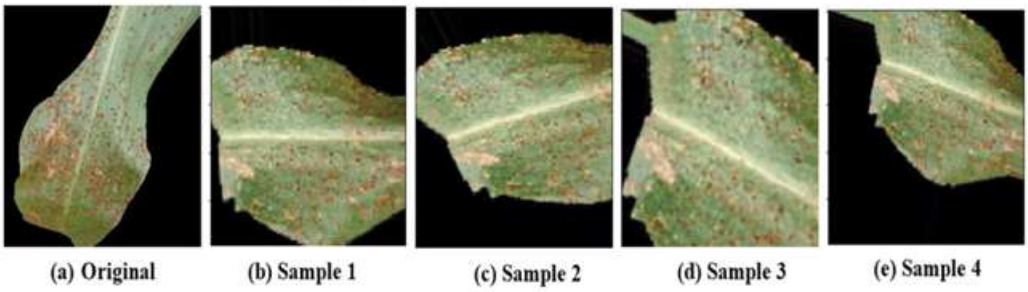

Fig. 4 Following the enhancement process, a typical rust image was produced. The original common rust image is shown in (a), and the images produced haphazardly utilizing some of the data augmentation approaches are shown in (b–e).

4.1 Result analysis

The suggested Neural Network model with several epochs that carry out an approximation function is used to estimate themean squared error. The number of validation sets is used to normalise the estimated errors throughout the validation procedure. The discrepancy between simulated as well as actual values is given by MSE. The MSE across training epochs, where the steadily decreasing values confirm effective learning of disease features, making the model suitable for real-time agricultural applications. Optimal validation criteria and the number of iterations are displayed in Fig. 5. At epoch 4, the optimal validation performance of suggested system is 0.50666. It indicates that the outcome would be stable following epoch 4. The gradient coefficient varies in the training state according to the number of iterations or epochs. At epoch 10, the gradient coefficient's ultimate value is 0.061239, or close to zero. The training and testing criteria will be better if the gradient coefficient has a minimum value. The gradient and validation check are displayed in Fig. 6. Gradient values are found to decline with a rise in the number of epochs. Number of iterations will be finished when the validation check at epoch 10 equals 6.

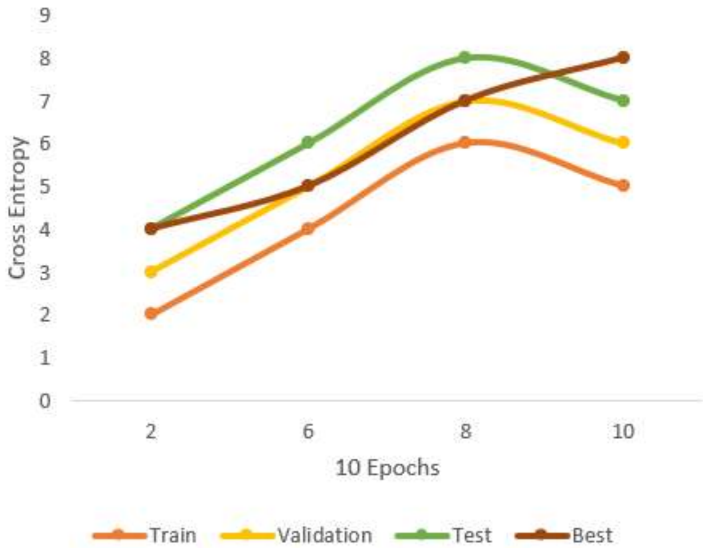

Fig. 5 Mean square error plot

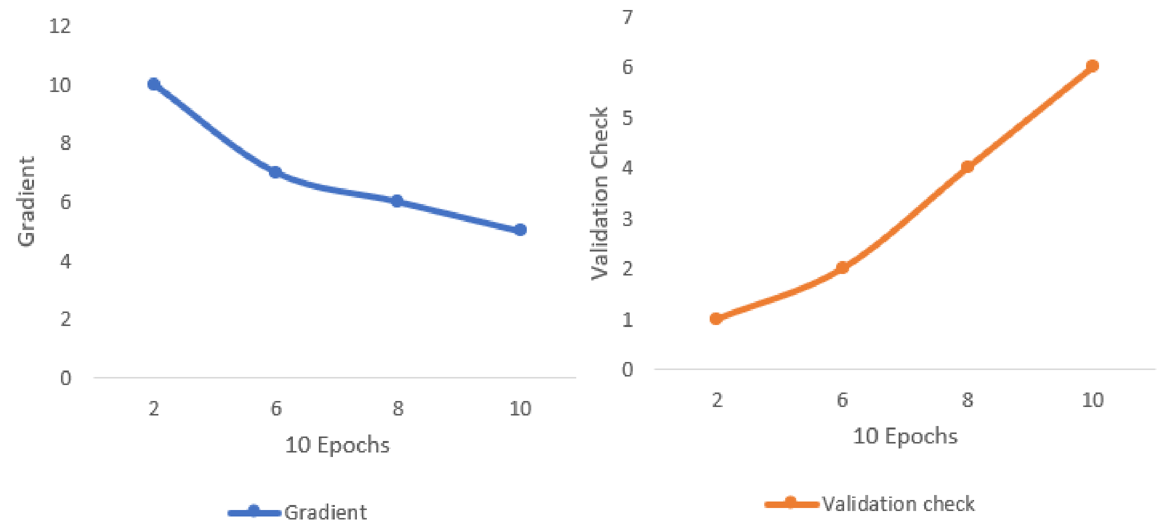

Fig. 6 Gradient and validation check

The ROC curves illustrate model performance across testing, validation, and overall datasets, showing improved classification ability with reduced false positive rates and increased true positive rates, suggesting effective disease detection in Fig. 7. The dataset was trained, tested, and validated using ROC plotting. Where the area is divided in half by the landslip slope, as indicated by the dotted lines in Fig. 5. The accuracy of a valuation indicator is determined by its range, with a maximum of 0.7 to 1 indicating excellent precision.

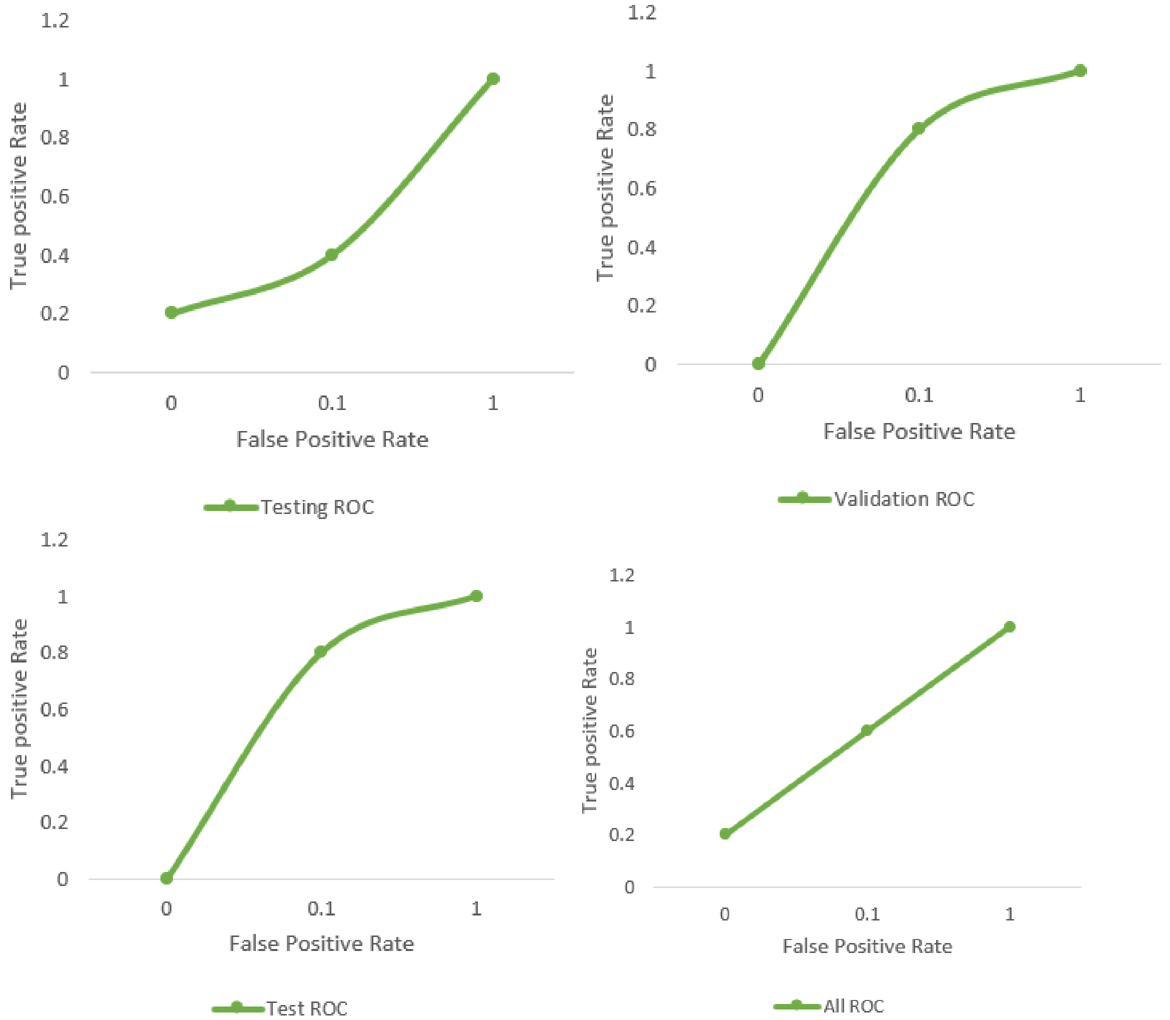

Fig. 7 ROC performance evaluation

Training accuracy precisely reflects how effectively the method is learning. In contrast, the validation accuracy predicts the generalisability of the model using a hold-out validation dataset. Suggested model's training as well asprecision and loss of validityare shown in Fig. 8. Although there was little fluctuation throughout validation test, loss curve shows that training and validation losses dropped over time and that there was little interval between them over the experiments. The proposal's training accuracy and lossas well as validation are displayed in Fig. 8

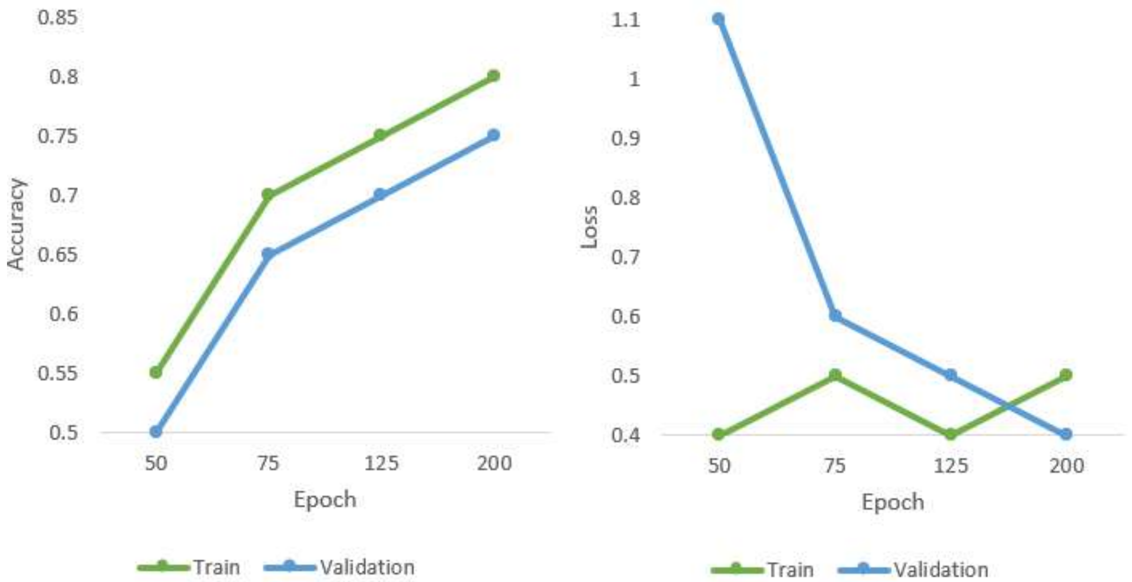

Fig. 8 Training and validation (accuracy and loss)

Table 5 comparative analysis between proposed and existing model

Model	Testing accuracy (%)	Precision (%)	Recall (%)	F1score (%)
Sequential	98.60	96.83	98.70	97.68
VGG16	92.39	93.55	94.51	95.71
VGG19	96.15	96.42	97.06	96.60
ResNet50	98.99	98.96	99.05	98.98
EFT_PSO_LM	99	98.99	99.71	99.99

The summary results, taking into account the experiment's recall, f1-score, accuracy, and precision, are shown in Table 5. It is also evident from the table that EFT_PSO-LM performs better than any other model. 5-fold cross-validation strategy on individually experiment when working with EFT_PSO-LM model in order to more accurately validate the experiment via EFT_PSO-LM is utilized. Consequently, in that scenario, 20% ofthe Data is utilized to test, and stay Eighty percent is used for training scenarios.

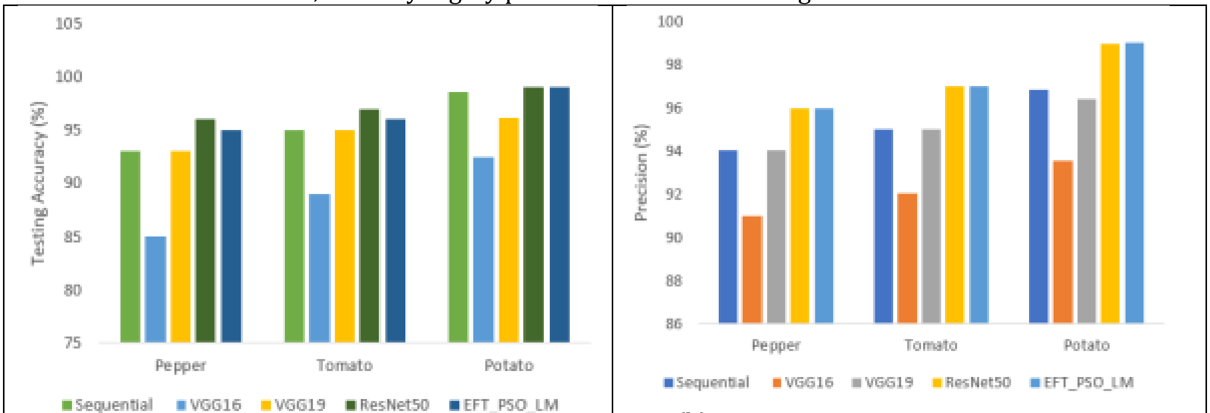

(a) Accuracy

(b) Precision

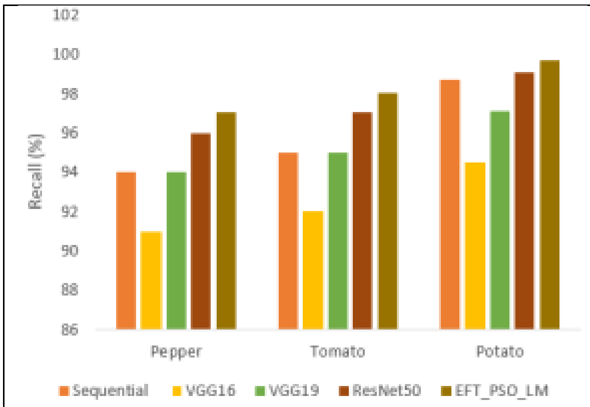

(c) Recall

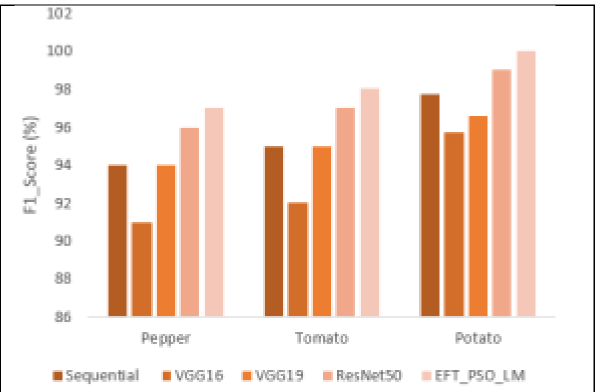

(d) F1_Score

Fig. 9 comparative analysis between proposed and existing model for (a) Accuracy, (b) Precision, (c) Recall, (d) F1-Score

Overview of several leaves taking into account each method accuracy performance during course of three experiments is displayed in Fig. 9. Accuracy (%) represents the percentage of correctly classified plant leaf disease images among the total samples. Fig 9(a) shows that EFT_PSO_LM achieved 99% accuracy, outperforming ResNet50 (98.99%), Sequential (98.60%), VGG19 (96.15%), and VGG16 (92.39%), confirming superior classification reliability. Precision (%) measures the proportion of correctly identified diseased leaves among all predicted diseased leaves. Fig 9(b) shows that the proposed EFT_PSO_LM achieved 98.99% precision, outperforming Sequential (96.83%), VGG16 (93.55%), VGG19 (96.42%), and ResNet50 (98.96%) in accurate disease classification. Recall (%) measures the model's ability to correctly identify all actual positive disease cases. Fig 9(c) shows recall values, where EFT_PSO_LM (99.71%) outperformed ResNet50 (99.05%), Sequential (98.70%), VGG19 (97.06%), and VGG16 (94.51%), ensuring superior disease detection sensitivity.F1-score (%) is the harmonic mean of precision and recall, balancing classification accuracy performance. Fig 9(d) shows the proposed EFT_PSO_LM model achieved the highest F1-score of 99.99%, outperforming ResNet50 (98.98%), Sequential (97.68%), VGG19 (96.60%), and VGG16 (95.71%).

4.2 Discussions

The discussion highlights limitations of earlier studies, emphasizes achieved improvements, compares results, and establishes the proposed research as a superior, and reliable for accurate plant disease detection. Early image processing methods required manual feature extraction, were highly sensitive to lighting/background variations, and lacked scalability for real-world applications [7–10].Traditional ML models relied on handcrafted features, struggled with overlapping/subtle symptoms, and degraded under noisy field conditions [18,19].Advanced feature-based models suffered from computational inefficiency, dependence on carefully designed features, and poor generalization in uncontrolled agricultural environments [20].Sequential networks showed limited depth and struggled with complex disease patterns, reducing generalization in large-scale datasets.VGG16 and VGG19 achieved good accuracy but faced high computational cost, vanishing gradient issues, and poor efficiency in real-time detection scenarios.ResNet50 improved feature extraction but exhibited training complexity, higher resource demands, and limited adaptability to highly diverse field conditions. The suggested EFT_PSO_LM model provides dependable plant disease diagnosis for precision farming and sustainable crop management through strong feature extraction, increased accuracy, computational efficiency, less overfitting, scalability, and adaptability. This research surpassed all previous methods by achieving a higher accuracy, a higher efficiency measure, and scalability to any number of devices in a framework where EFT_PSO_LM can be viewed as the best framework. The proposed model's high accuracy and reliability enable early disease detection, reducing crop losses and unnecessary pesticide use. Farmers and agronomists can implement timely interventions, optimize resource allocation, and enhance sustainable farming practices. Integration into real-time monitoring systems can improve overall crop health management and support precision agriculture initiatives.

5. Conclusion

Plant diseases continue to pose a significant challenge to global food security, necessitating timely and accurate detection methods. This study aimed to develop an enhanced image-based framework for plant disease identification by integrating robust feature extraction and hybrid optimization-driven classification techniques. The proposed model combined EFT for extracting discriminative leaf features with PSO and LM algorithms for efficient classification. Experimental results demonstrated that the framework achieved high performance, with accuracy, precision, recall, and F1-score exceeding 99%, outperforming existing state-of-the-art approaches. These results demonstrate the efficacyof the model in facilitating rapid disease identification, supporting early intervention, improved crop management, and sustainable agricultural productivity. Despite these promising results, limitations remain, including dependency on high-quality images and potential challenges in generalizing to new plant species or diverse environmental conditions.Extending the framework to manage bigger and more varied datasets should be the main goal of future research, integrating real-time field deployment with IoT and mobile technologies, and exploring additional DL and hybrid optimization techniques to further enhance detection accuracy and robustness in practical agricultural settings.

Reference:

1. Kusuma S, Jothi KR (2024) Early betel leaf disease detection using vision transformer and deep learning algorithms. Int J Inf Technol 16:169–180.
2. Sujatha R, Suresh P (2025) Advancing plant leaf disease detection by integrating machine learning and deep learning techniques. Sci Rep 15:12345. https://doi.org/10.1038/s41598-024-72197-2
3. Mahadevan K, Punitha A, Suresh J (2024) Automatic recognition of rice plant leaf diseases detection using deep neural network with improved threshold neural network. E-Prime Adv Electr Eng Electron Energy 8:100534.
4. Shoaib M (2023) An advanced deep learning models-based plant disease detection: A review of recent research. Front Plant Sci 14:1158933. https://doi.org/10.3389/fpls.2023.1158933
5. Simhadri CG, Kondaveeti HK (2023) Automatic recognition of rice leaf diseases using transfer learning. Agronomy 13:961. https://doi.org/10.3390/agronomy13040961
6. Reis HC, Turk V (2024) Potato leaf disease detection with a novel deep learning model based on depthwise separable convolution and transformer networks. Eng Appl Artif Intell 133:108307.
7. Fang K, Liu X, Zhang Y (2025). RLDD-YOLOv11n: Research on rice leaf disease detection and classification using deep learning. Agronomy 15:1266. https://doi.org/10.3390/agronomy15061266
8. Bonkra A, Pathak S, Kaur A, Shah MA (2025) Machine learning-based real-time detection of apple leaf diseases: An enhanced pre-processing perspective. Int J Comput Digit Syst 17:1–14. https://doi.org/10.12785/ijcds/1571032285
9. Mohammed MA, Lakhan A, Abdulkareem KH, Almujally NA, Al-Attar B, Memon S, et al. (2024) Edge-cloud remote sensing data based plant disease detection using deep neural networks with transfer learning. IEEE J Sel Top Appl Earth Obs Remote Sens.
10. Thite S, Suryawanshi Y, Patil K, Chumchu P (2024) Sugarcane leaf dataset: A dataset for disease detection and classification for machine learning applications. Data Brief 53:110268.
11. Liu H, Zhang Y, Li X (2023) Deep convolutional neural networks for real-time tomato leaf disease detection. Comput Electron Agric 210:107925. https://doi.org/10.1016/j.compag.2023.107925
12. Ahmed I, Yadav PK (2024) Predicting apple plant diseases in orchards using machine learning and deep learning algorithms. SN Comput Sci 5:700.
13. Paul H, Ghatak S, Chakraborty S, Pandey SK, Dey L, Show D, Maity S (2024) A study and comparison of deep learning based potato leaf disease detection and classification techniques using explainable AI. Multimed Tools Appl 83:42485–42518.
14. Demilie WB (2024) Plant disease detection and classification techniques: a comparative study of the performances. J Big Data 11:5.
15. Wang J, Li Y, Chen S (2023) Comparative analysis of ResNet50 and Inception-v3 for automated plant disease classification using leaf images. Comput Electron Agric 209:107890. https://doi.org/10.1016/j.compag.2023.107890
16. Jha P, Dembla D, Dubey W (2024) Deep learning models for enhancing potato leaf disease prediction: Implementation of transfer learning based stacking ensemble model. Multimed Tools Appl 83:37839–37858.
17. Al-Shahari EA, Aldehim G, Aljebreen M, Alqurni JS, Salama AS, Abdelbagi S (2024) Internet of Things Assisted Plant Disease Detection and Crop Management using Deep Learning for Sustainable Agriculture. IEEE Access.
18. Qadri SAA, Huang NF, Wani TM, Bhat SA (2024) Advances and challenges in computer vision for image-based plant disease detection: a comprehensive survey of machine and deep learning approaches. IEEE Trans Autom Sci Eng.

19. Khan S, Iqbal MM, Shah M (2023) Real-time detection and classification of tomato leaf diseases using deep convolutional neural networks. Comput Electron Agric 209:107884. https://doi.org/10.1016/j.compag.2023.107884
20. Zhang Y, Li X, Wang H (2023) Deep learning-based detection and classification of plant leaf diseases for precision agriculture. Comput Electron Agric 210:107928. https://doi.org/10.1016/j.compag.2023.107928
21. Eunice J, Popescu DE, Chowdary MK, & Hemanth J (2022) Deep learning-based leaf disease detection in crops using images for agricultural applications. Agronomy, 12(10), 2395. https://doi.org/10.3390/agronomy12102395
22. Saleem MH, Potgieter J, & Arif KM (2022) A performance-optimized deep learning-based plant disease detection approach for horticultural crops of New Zealand. IEEE Access, 10, 89798–89822. https://doi.org/10.1109/ACCESS.2022.3205042
23. Moupojou E, Tagne A, Retraint F, Tadonkemwa A, Wilfried D, Tapamo H, & Nkenlifack M (2023) FieldPlant: A dataset of field plant images for plant disease detection and classification with deep learning. IEEE Access, 11, 35398–35410. https://doi.org/10.1109/ACCESS.2023.3270096